UNIZIK JOURNAL OF ENGINEERING AND APPLIED SCIENCES (UJEAS)

Research Article

Determination of performances of natural organic polymers for colour removal from simulated wastewater: Coagulation-adsorption kinetics and mathematical modelling approach

Ifeoma Amaoge Obiora-Okafo, Okechukwu Dominic Onukwuli, Monday Omotioma, Chinyere Blessing Ezekannagha, Jerome Undiandeye, Ifeanyi Omezi, Chinenyenwa Nkeiruka Nweke.

Special Issue
A Themed Issue in Honour of Professor Onukwuli Okechukwu Dominic (FAS).

This special issue is dedicated to Professor Onukwuli Okechukwu Dominic (FAS), marking his retirement and celebrating a remarkable career. His legacy of exemplary scholarship, mentorship, and commitment to advancing knowledge is commemorated in this collection of works.

Edited by
Chinonso Hubert Achebe PhD.
Christian Emeka Okafor PhD.

UJEAS

UNIZIK JOURNAL OF ENGINEERING AND APPLIED SCIENCES

UNIZIK Journal of Engineering and Applied Sciences 4(1), March (2025), 1763-1783
Journal homepage: https://journals.unizik.edu.ng/index.php/ujeas
PRINT ISSN: 2992-4383 || ONLINE ISSN: 2992-4391

Determination of performances of natural organic polymers for colour removal from simulated wastewater: Coagulation-adsorption kinetics and mathematical modelling approach

Ifeoma Amaoge Obiora-Okafo*[1], Okechukwu Dominic Onukwuli[1], Monday Omotioma[2], Chinyere Blessing Ezekannagha[3], Jerome Undiandeye[4], Ifeanyi Omezi[5], Chinenyenwa Nkeiruka Nweke[1]

[1]Department of Chemical Engineering, Nnamdi Azikiwe University, Nigeria
[2]Department of Chemical Engineering, Enugu State University of Science and Technology, Nigeria
[3]Department of Chemical Engineering, Madonna University, Nigeria
[4]Department of Chemical Engineering, University of Port Harcourt, Nigeria
[5]Department of Petroleum Engineering, Nnamdi Azikiwe University, Nigeria
[*]**Corresponding author:** ia.obiora-okafo@unizik.edu.ng

Abstract

In this study, coagulation-flocculation efficiencies of Natural organic polymers (NOPs) were evaluated for the decolourisation of anionic synthetic dye in wastewater. The proximate composition, structure, and surface morphology of the *Brachystegia eurycoma* coagulant (BEC) and *Vigna subterranean* coagulant (VSC) were analysed using standard official methods, Fourier-Transform Infrared (FTIR) spectroscopy, and scanning electron microscopy (SEM), respectively. The order of removal efficiency was VSC > BEC with an optimum of 97.7% and 82.0% respectively, at pH 2, 200 mgBECL^{-1} and 200 mgVSCL^{-1} coagulant dosage, 100 mgL^{-1} dye concentration, 480 min, and 303 *K*. The values of *K* and α obtained for BEC and VSC were 1.65 E-02 Lmg^{-1}min^{-1}, 1.2 and 1.76 E-04 L/mg^{-1}min^{-1}, 2.2 respectively. The coagulation time (T_{ag}) of 22.42 min and 27.92 min for BEC and VSC respectively as deduced from the plot showed a rapid coagulation process. The kinetics of coagulation-flocculation demonstrate that the process conforms with a pseudo-second order model with correlation coefficient $R^2 > 0.990$, suggesting that chemisorption is the rate-controlling phase. It also reveals that particle adsorption on polymer surfaces occurs mostly as a monomolecular layer. The experimental data was well predicted by the cross-validation test, with mean relative deviation modulus (*M%*) of 0.223% and 1.829% for BEC and VSC, respectively. In conclusion, the coagulants studied added meaningful progress in wastewater treatment via coagulation-flocculation while showing significant adsorption features. Additionally, the application of kinetics and modelling in separation processes involving particle transfer should be considered a prerequisite in water treatment processes.

Keywords: Coagulation-flocculation; Biebrich Scarlet (AR 66); natural organic polymers; coagulation-adsorption kinetics; particle transfer.

1. Introduction

In a colloidal state, dye wastewater comprises of large amounts of colour particles, heavy metals, surfactants, organic and inorganic matters, which have adverse effects on human health, possibly causing skin diseases and respiratory problems (Ishak et al. 2020; Obiora-Okafo et al. 2019). Coagulation-flocculation is classified as one of the most efficient methods widely used for colour removal from wastewater because of its efficiency, cost-effective, and ease of operation. Coagulation is the process of destabilization of aqueous particles initially present in a suspension by the addition of a coagulant (natural or synthetic), so that the charged particles are neutralized to enable them to be attracted to each other to form settleable flocs. Aqueous particles generally have a net negative charge, thereby repelling one another. In addition, aqueous particles (1 nm – 1 μm) generally do not settle at all or

without assistance in a reasonable time. Therefore, the surface charge of particles can be reduced or destabilized by adding a coagulant carrying an opposite charge (Liang et al. 2016). Commonly used coagulants are inorganic salts such as Al(SO4)3 or FeCl3, as well as synthetic organic polymers. Although these chemicals are effective in removing dyes and other contaminants from wastewater, several disadvantages have recently been discovered, such as their impact on human life, with diseases such as Alzheimer's disease being associated with certain inorganic salts, and neurotoxins being associated with acrylic amid (Kim et al. 2022).

Numerous research have been carried out on the elimination of these pollutants before discharge, employing natural organic polymers (NOPs) in the coagulation-flocculation process (Igwegbe and Onukwuli 2019; Kim et al. 2022; Onukwuli and Obiora-Okafo 2019). The world's awareness on environmental sustainability has shifted many researchers to adopt natural polymer coagulants (including plant-based or animal-based) as an alternative for wastewater treatment due to their benefits over chemical coagulanting agents, particularly their low toxicity, low residual sludge production, cost-effectiveness and biodegradability (Igwegbe and Onukwuli 2019; Obiora-Okafo and Onukwuli 2018b).

Proper selection of natural coagulant promotes large flocs formation which brings a rapid settling through various mechanisms such as adsorption of particles, charge neutralisation, sweep flocculation, and inter-particle bridging (Igwegbe et al. 2021b; Ndagijimana et al. 2024). Adsorption mechanism is common when NOPs are used as a coagulant due to their polymeric features including extending loops and tails (Ibrahim et al. 2021). Hence, NOPs enhance flocs size by attracting smaller particles to generate much larger flocs. When there is some affinity between polymer segments and particle surfaces, particles interact through adsorption which occurs through electrostatic forces, hydrogen bonding, as well as ionic bonding. Most NOPs might be anionic, cationic or non-ionic in nature (Ibrahim et al. 2021).

This work is focused on employing *Brachystegia eurycoma* seed *and Vigna unguiculata* seed as NOPs precursors for the treatment. *Brachystegia eurycoma* seed belongs to the *Caesalpiniaceae* family with average contents of 15% crude fat, 2.9% crude fiber, 20% protein, 56% carbohydrate, and 4.5% ash (Aviara et al. 2014). The seeds are good source of bioactive compounds comprising of flavonoids, alkaloids, phenolic compounds, saponins, tannins, protein, carbohydrate, lipid, and fibre. Crude extract from *Brachystegia eurycoma* seed flour is non-toxic, biodegradable organic polymer of high molecular weight of 5-19KDa (Aviara et al. 2014).

Vigna subterranean (also known by its common names Bambara groundnut, Bambara bean or hog - peanut, is a member of the family fabaceae. Because of their relatively high protein content, *Vigna subterranean* seeds are a potentially valuable protein source for all classes of livestock. *Vigna subterranean* protein is one of the important sources of vegetable protein due to its high nutritional value. The seed makes a complete food, as it contains sufficient quantities of proteins, carbohydrates and lipids (Atoyebi et al. 2017). From previous study by Halimi et al (Halimi 2020), the molecular weight of the protein extract from *Vigna subterranean* seed flour is of the range 17-22KDa and the protein content was said to be cationic peptides. However, it has been recommended to use the shells and other by-products to feed animals and to use the seeds as food so that people can benefit from their protein. The essential amino acid profiles of the seeds are comparable to that of soybean.

The study of kinetics of coagulation-floculation is highly significant in the area of colloid science because it is used to investigate the colloidal and hydrodynamic interactions involved in particle-particle contacts. Coagulation-floculation kinetics have been investigated using variety of methods including such as (1) Direct counting of the coagulating colloids using an ultramicroscope, or a particle counter, probably yields the most clear-cut results. However, because this method is time-consuming, it is not ideal for routine coagulation kinetics analysis (Li et al. 2024). (2) Bulk technique approach is a frequently utilized procedure for coagulation-flocculation kinetics because it monitors changes in the particle suspension with time (Obiora-Okafo et al. 2020). This time dependent approach offers rapid operation, easy to use, cost effective and suitable for multi-particle determination.

The dynamics of coagulation rate addresses how rapidly or slowly a suspension of particles will coagulate. Coagulation rate has immense practical implications and it plays an important role in the mathematical modelling, design and control of water and wastewater treatment plants. Smolukwoski was the foremost scientist to study the rate of coagulation of spherical particles due to Brownian motion, taking diffusion coefficient of particles as constant (Hyrycz et al. 2022).

Mathematical model is a set of variables and equations, mostly time-dependent, that establish relationships between the variables that represent a system. It may be used to simulate dynamic behavior, investigate control mechanisms, and create a coagulation-flocculation process. Modelling of the process improves and optimises the design of equipment and develops a better insight on the process operation (Obiora-Okafo et al. 2020). The prediction of particle reduction rate in response to a set of coagulation circumstances is an area of interest in the theoretical study of the coagulation-flocculation process. Brownian mode of collisions on a spherical target would be analysed in more detail since it captures the crucial kinetics of various mass transfer processes such as coagulation-flocculation, adsorption methods, and advanced oxidation practices.

In this study, the possibility of employing active protein components extracted from bio-coagulants for colour removal from dye containing aqueous solution is investigated. Effectively, cationic biocoagulants and anionic dye were selected for high-performance jar testing, based on their ionic composition. Characterisation and fibre-metric studies of the precursors were performed. The newer approach of extracting active coagulant agent was adopted in the coagulation-flocculation process. Spectrophotometry analysis was used to observe the dynamic behaviour of particle concentrations at optimal conditions. The study also explores adsorption capacities of the coagulants, the kinetics of particle transfer, and used modelling to predict the real-time particle transfer rate during the coagulation-flocculation process.

2.0 Materials and methods

2.1 Coagulant Preparation and Extraction of Active Component

Dried seeds of *Brachystegia eurycoma* and *Vigna subterranean* as shown in **Fig. 1** were purchased from Enugu, Nigeria. Developed seeds with no signs of ageing were used. The dry seeds were ground (63 – 600 µm) using a food processor (Model BL 1012, Khind) to accomplish solubilisation of active constituents. Samples (2 g) were prepared using distilled water of 0.5 M NaCl solution, stirred for 20 min using Magnetic stirrer (Model 78HW - 1, U-Clear England) and filtered through Whatman paper No. 125 mm diameter, to enable visible nano, micro, and macro-particles to be present in the filtrate for enhanced coagulation-flocculation. The filtrate is labelled the crude extract, used as the coagulants at the required dosages. A s required, fresh solutions were prepared frequently and kept refrigerated (Onukwuli and Obiora-Okafo 2019; Sonal et al. 2021).



Fig. 1. Dried seeds of a) *Brachystegia eurycoma*, and b) *Vigna subterranean*

2.2 Characterisation of the Coagulants

Proximate parameters including yield, bulk density g/mL, moisture contents (%), ash contents (%), protein contents (%), fat contents (%), carbohydrate contents (%), and fibre contents (%) of the seed powders were analyzed by the standard official methods of analysis of the Association of Official Analytical Chemists (Vivas et al. 2025). The chemical structure and functional groups were investigated using an FTIR spectrophotometer provided by IR Affinity-1, Shimadzu Kyoto, Japan. The spectra range were between 4000 – 400 cm^{-1}. Surface structures, morphologies and pore distribution analysis were performed using a scanning electron microscope, provided by Phenom Prox., world Eindhoven, Netherlands) and the images were presented after 3D reconstruction using ImageJ v1.53 (Ighalo et al. 2021) at ×600 magnification.

2.3 Preparation of Synthetic Wastewater

AR 66 was manufactured by May & baker, England having a molecular structure and physical characteristic as shown in **Fig. 2a** and **Table 1** respectively. To obtain the absorption spectrum of the dye, 1000 mg/L of AR 66 was dissolved in distilled water. The solution was scanned against the blank (distilled water) in the range of 200-850 nm using UV-vis spectrophotometer (Shimadzu, Model, UV - 1800). Also, similar amount of AR 66 was prepared as stock solution in accurately weighed amounts and kept in separate doses. The working concentrations of 10-100 mg/L were prepared from the stock solution using the dilution method (Onukwuli et al. 2019). The wavelength obtain at maximum absorbance (λ_{max}) is shown in **Fig. 2b**.

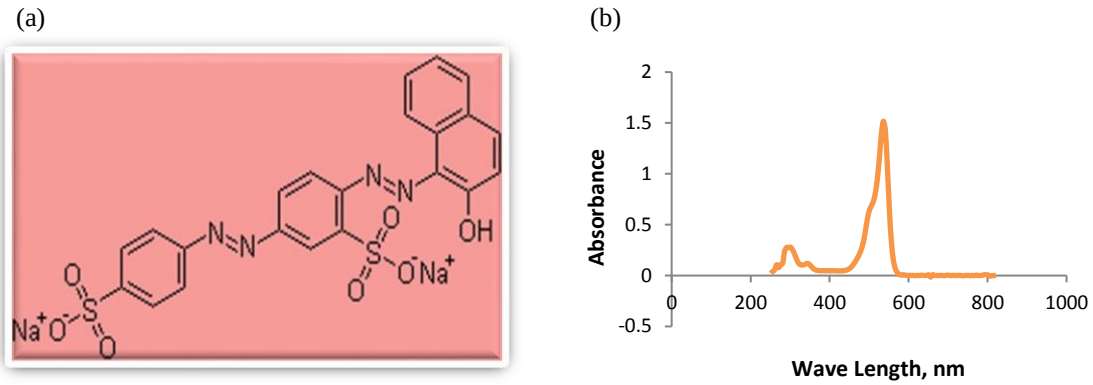


Fig. 2. (a) Structure of AR 66, (b) Spectrum report for AR 66

Table 1: Physical properties of Biebrich Scarlet

Property	Data
Chemical Name	Sodium 6- (2-hydroxyna phthylazo) – 3, 4' – azodibenzenesulfonate
Chemical formula	$C_{22}H_{14}N_4Na_2O_7S_2$
Molecular Weight	556.48
CAS number	4196 – 99 – 0
ECC number	224 – 084 - 5
Melting point	181 - 188^{0}C.
UV /visible Absorbance	Max (water): 505+ 6nm.
C.I number and name	26905 / Acid Red 66
Class	Azo
Common name	Biebrich Scarlet.

2.4 Coagulation Assay

The coagulation activity of the seed extracts were determined by Jar test which evaluates the coagulation activities of the active proteins extracts from the precurors (Obiora-Okafo and Onukwuli 2018a). The jar test procedure was carried out experimentally using Phipps and Bird, VA, USA apparatus, which involves 4 min of rapid mixing speed at 100 rpm and slow mixing speed of 40 rpm for 25 min. The suspensions were allowed to settle for 480 min, clarified samples from the beakers were collected for absorbance analysis using a UV-VIS spectrophotometer at λ_{max} of 531 nm. A preliminary test was conducted to establish the optimum factors including pH, coagulant dosage (mg/L), dye concentration (mg/L), settling time (min), and temperature (K). The pH was adjusted to the desired value using 0.1 M HCl and 0.1 M NaOH.Then, The measurement of colour concentration (mg/L) was made by comparing absorbance to concentration on a calibration curve. (Obiora-Okafo et al. 2018), while the colour removal efficiencies were calculated according to **Eq. (1)** (Obiora-Okafo and Onukwuli 2018a).

$$\text{Colour removal (\%)} = \left(\frac{C_0 - C}{C_0}\right) x\ 100 \qquad (1)$$

where, C_o and C represent the initial and final colour concentrations (mg/L) before and after the process, respectively.

2.5 Theoretical Principles Guiding Coagulation-Flocculation Kinetics

Movement of spherical particles in mass transfer operations cannot be effectively studied without involving kinetics. Kinetics could be used to study the hydrodynamic spherical particle-particle interactions. Therefore, coagulation-flocculation involves two particles of comparable size colliding with one another; leading to the formation of doublets, triplets, etc. (Ghernaout et al. 2015a).

On that note, coagulation kinetics of spherical-particle contact was studied in this section following the Brownian diffusion mechanism (Peri-kinetics). Hence, Smoluchowski's model which has formed the basic of virtually all later researches in coagulation-flocculation modelling was adopted (Bal 2020). Flocculation of particles for full aggregate formations may not be defined as a second-order process as recorded earlier by some researchers. However, Von Smoluchowski theory and Brownian coagulation kinetics equation of single-disperse particles are employed to deduce the coagulation rate constant and order of the reaction. The equation describing the aggregation kinetics is given in **Eq. (2)** .

$$\frac{-dC}{dt} = -kc^{\alpha} \quad (2)$$

where C presents the concentration of the primary particles; α is the coagulation-flocculation reaction order; K is rate constant. Linearizing **Eq. (2)** gives **Eq. (3)** (Ugonabo et al. 2020).

$$\ln\left(\frac{-dc}{dt}\right) = \ln k + \alpha \ln C \quad (3)$$

Hereafter, a plot of $ln\ (\frac{-dC}{dt})$ versus $(\ln C)$ gives a straight line, deducing K and α, from the intercept and slope, respectively. In addition, the rate constant could be calculated from Brownian hydrodynamics as shown in **Eq. (4)** (Ghernaout et al. 2015a).

$$k = \frac{8K_BT}{3\mu} \quad (4)$$

Where K_B is the Boltzmann's constant (J/ K), T is the absolute temperature (K) and μ is the viscosity of the medium. The equation describing the timed-based evolution of the flocs clusters is shown as **Eq. (5)** .

$$\frac{dC_k}{dt} = \frac{1}{2}\sum_{i=1}^{k-1} k_{ij}C_iC_j - C_k\sum_{i=1}^{\infty} k_{ik}C_i \quad (5)$$

where $\frac{dC_k}{dt}$ is the rate at which particle concentration changes; the coagulation constant k_{ij} is determined by collisions between i and j particles, yielding (k-i) mer. This kernel represents the mutual diffusion coefficient (D_{ij}) and collision radius of the sphere (R_{ij}) of the meeting of i-mer and j-mer, as well as their reliance on i and j. Through this process, the coagulation constant, $k_{ij} = k_1$ assuming a constant kernel, **Eq. (6)** (Ugonabo et al. 2020).

$$k_1 = 8\pi RD \quad (6)$$

where, K_1 represents the Von Smoluchowski's rate constant showing rapid coagulation, R is the radius of the particles and D is the diffusion coefficient of the particles according to Brownian motion. Therefore, relating Von Smoluchowski rate constant to Stokes-Einstein (SE) diffusion coefficient for translational diffusion , gives an expression such as **Eq. (7):**

$$k_1 = \frac{4}{3}\frac{K_BT}{\mu} \quad (7)$$

Combination of **Eqs. (4)** and **(7)** yields **Eq. (8):**

$$k = 2k_1 \quad (8)$$

Particle-particle collisions bring about flocculation, thus resulting to the reduction in the total number of particles. Hence, the rate of flocs growth is generally determined by the rate of these collisions. Centered on the work of Von Smoluchowski as reported by Oke et al (Oke et al. 2021), it is evidenced that the frequency f_{ij} of twofold collision between particles of type i and j is specified in **Eq. (9)** .

$$f_{ij} = \beta(v_i, v_j)C_iC_j \tag{9}$$

where C_i and C_j are the concentrations of two particle types. $\beta\ (v_i, v_j)$ shows the collision frequency factor. The rate at which particles of size k is formed per unit volume by their collisions of size i and j is given by **Eq. (10)** .

$$\frac{1}{2}\sum_{i+j=k} f_{ij} \tag{10}$$

The ½ factor in **Eq. (10)** implies that each collision is computed double in the summation. **Eq. (10)** is as a result of the generation of the k^{th} species. In addition, particle k collides with other particles leading to larger volume particle, v_k. **Eq. (11)** gives the disappearing term as (Oyegbile et al. 2016).

$$\sum_{i=1}^{\infty} f_{1k} \tag{11}$$

The overall balance equation for k^{th} species is given by **Eq. (12)** (Oyegbile et al. 2016).

$$\frac{dC_k}{dt} = \frac{1}{2}\sum_{i=1;i+j=k}^{i=k-1} f_{ij} - \sum_{i=1}^{\infty} f_{1k} \quad \text{for } k = 1,2,3,\ldots\ldots\infty \tag{12}$$

Using **Eq. (9)**, **Eq. (12)** becomes **Eq. (13) (Obiora-Okafo et al. 2019).**

$$\frac{dC_k}{dt} = \frac{1}{2}\sum_{i=1;\, i+j=k}^{i=k-1} \beta_{ij}C_iC_j - C_k \sum_{i=1}^{\infty} \beta_{ik}C_i \tag{13}$$

where $\beta ij = \beta\ (vi, vj)$.

Including the collision efficiency factor, **Eq. (9)** is substituted by **Eq. (14)**

$$f_{ij} = E_{ij}\beta C_iC_j \tag{14}$$

where E_{ij} is the efficiency element for collision between i and j particles, f_{ij} is the rate at which particles i and j collides. Therefore, the collision frequency for Brownian motion, is specified as **Eqs. (15)-(16)** .

$$\beta(v_i = v_j)\frac{8K_BT}{3\mu} = k \tag{15}$$

$$\beta(v_i = v_j)\frac{E8K_BT}{3\mu} = k \tag{16}$$

Relating to **Eqs. (4)**, **(15)** and **(16)**, brings about another relationship between collision frequency and Von Smoluchowski rate constant as shown through **Eqs. (17)-(19)** .

$$\beta = 2k_1 \tag{17}$$

also, $$\beta = 2Ek_1 \tag{18}$$

and $$E = \frac{\beta}{2K_1} \tag{19}$$

The population balance of **Eq. (13)** as compared with **Eq. (16)**, gives **Eq. (20)**

$$\frac{dC_k}{dt} = \frac{k}{2}\sum_{i=1;i+j=k}^{i=k-1} C_iC_j - kC_k \sum_{i=1}^{\infty} C_i \tag{20}$$

Therefore, the total concentration of particles in a closed system, giving at time, t is **Eq. (21)**

$$C_{tot}(t) = \sum_{i=1}^{\infty} \mathrm{C_i} \quad (21)$$

The summation of **Eq. (20)**, overall particles $K = 1, 2, 3, \ldots\ldots, \infty$, yields **Eq. (22)** as

$$\frac{dC_{tot}}{dt} = \frac{\mathrm{K}}{2} \sum_{k=1}^{\infty} \sum_{i=1; i+j=k}^{i=k-1} C_i C_j - \mathrm{k} C_{tot}^2 \quad (22)$$

The first term on the right side of **Eq. (22)** is given by $(\frac{k}{2}) C_{tot}^2$, which leads to **Eq. (23)**

$$\frac{dC_{tot}}{dt} = \frac{-\mathrm{k}}{2} C_{tot}^2 \quad (23)$$

Brownian coagulation is similar to the second-order reaction kinetics as shown in **Eq. (23)**. Giving the conditions of $C_{tot} = C_o$ at $t = 0$ and integrating **Eq. (23)** gives **Eq. (24)** .

$$C_{tot}(t) = \frac{C_0}{1 + K C_0 \frac{t}{2}} \quad (24)$$

The decline in the the total number of particles with time is shown in **Eq.** (**24**), resulting to:

$$C_k(t) = \frac{C_0 (\frac{t}{T_{ag}})^{K-1}}{(1 + \frac{t}{T_{ag}})^{K+1}} \quad (25)$$

Then,

$$T_{ag} = \frac{2}{K C_0} = \frac{3\mu}{4 C_0 K_B T} \quad (26)$$

where T_{ag} is the characteristic time, also known as the coagulation time. The characteristic time shows the time it takes each particle concentration to halve (Obiora-Okafo and Onukwuli 2018b). Later stages of flocculation involves the formation of singlet, doublets, triplets, quadruplet, etc., thus, number of *k* - mers, could be solved using **Eq. (25)** to give **Eq. (27) - (30)** for each scenario (Obiora-Okafo et al. 2019).

$$C_1 = \frac{C_0}{(1 + \frac{t}{T_{ag}})^2} \quad (27)$$

$$C_2 = \frac{C_0 (\frac{t}{T_{ag}})}{(1 + \frac{t}{T_{ag}})^3} \quad (28)$$

$$C_3 = \frac{C_0 (\frac{t}{T_{ag}})^2}{(1 + \frac{t}{T_{ag}})^4} \quad (29)$$

$$C_4 = \frac{C_0 (\frac{t}{T_{ag}})^3}{(1 + \frac{t}{T_{ag}})^5} \quad (30)$$

2.6 Equation Guiding the Mathematical Modelling of Particle Transfer

Colloidal particles are brought into interactions following definite manners by Brownian diffusion (peri-kinetic agglomeration); fluid motion (orthokinetic agglomeration) and differential sedimentation as illustrated in **Fig. 3** (Ghernaout et al. 2015a). Brownian motion of particles suspended in water moves in random motion resulting to several collisions, giving rise to thermal energy. As a result of this, collisions among particles produce perikinetic aggregation, hence, it is more flexible to estimate the rate of the created collisions. Therefore, it is evident that Brownian agglomeration has less capacity to form larger aggregates. Practically, flocculation processes are

frequently accomplished under some conditions where the suspension is under the action of some definite amount of shear, such as by flow or stirring . Then, this application may generate greater influence on the rate of particle collisions, resulting to orthokinetic agglomeration (Bal 2020). As a result, the primary theoretical concept to this theory was a product of Smoluchowski's studies, together with their studies on perikinetic agglomeration. In orthokinetic collisions, Smoluchowski worked on spherical particles in uniform and laminar shear (Oke et al. 2019).

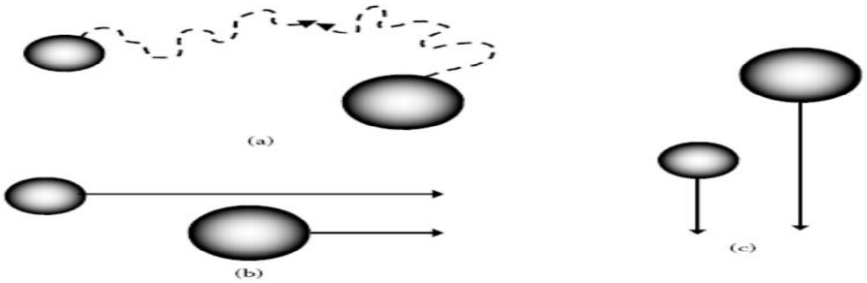


Fig. 3. Spherical particle collision transport showing: (a) Brownian diffusion; (b) fluid motion; and

(c) differential settling.

This study shows that the model equation examined describe the behaviour of the particle transfer in the direction of the adsorbing particles which is triggered by coagulation-flocculation. Going through the model, the following assumptions were well-thought-out; the basis of the model was governed and drawn from Fick's law, angular symmetry occurs for the particles, assuming a simple homogeneous system, assuming a single-dimensional particle transfer occurs, taking the process to be an isothermal, neglecting an external resistance to particle transport.

The diffusion coefficient, D is a relevant transport property in studying colloidal particle which represents the function of Brownian motion on particle transfer. Therefore, associating it with Fick's law is shown in **Eq. (31)** :

$$I = -D\frac{\partial C_i}{\partial_r} \tag{31}$$

where I is the diffusive flux of the particle, C_i is particle concentration and $\frac{\partial C_i}{\partial_r}$ is concentration gradient. Brownian motion-controlled diffusion is associated with the movement of particle from a region of higher concentration to a lower concentrated region (Li et al. 2024). A spherical particle transfer taking note of a microscopic system is shown in Fig. 4. By taking a material balance equation over a spherical shell, the basic differential equation for particle mass transfer is obtained .

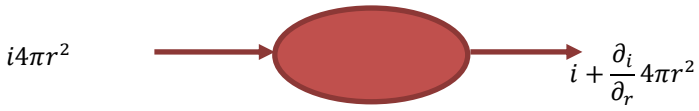


Fig. 4. Particle transfer considering a microscopic system

Time rate of change of particles = mass inflow of particles

- mass efflux particles (32)

Representing **Eq. (32)** mathematically, gives **Eq. (33)**

$$\frac{\partial (C_i) 4\pi r^2}{\partial t} = i4\pi r^2 - \left(i + \frac{\partial_i}{\partial_r}\right) 4\pi r^2 \tag{33}$$

Simplifying **Eq. (33)** gives **Eq. (34)**

$$\frac{r^2 \partial C_i}{\partial t} = -r^2 \frac{\partial_i}{\partial_r} \quad (34)$$

Joining **Eq. (34)** with **Eq. (31)** gives **Eq. (35)**

$$\frac{\partial C_i}{\partial t} = D \frac{1}{r^2} \frac{\partial}{\partial_r} (r^2 \frac{\partial C_i}{\partial_r}) \quad (35)$$

where C_i is the number of particle concentration; i, and r is the radius of the sphere. The equation describing the rate of particle transfer during the coagulation-flocculation process is a partial differential equation (**Eq. (35)**). It is also similar to the mass transfer to a sphere by . Replacing $C_j r^2$ for C, **Eq. (35)** turn out to be **Eq. (36)**

$$\frac{\partial C}{\partial t} = \frac{\partial}{\partial_r} D \frac{\partial C}{\partial_r} \quad (36)$$

For the initial condition in **Eq. (37)** .

$$C_i\ (t = 0, r)\ C_{io} \quad (37)$$

Also, the boundary conditions are **Eq. (38) - (39)**

$$C_i\ (r = 0, t)\ C_{io} \quad (38)$$

$$C_i\ (r = a, t)\ C_{eo} \quad (39)$$

where C_{eo} is the equilibrium particle concentration in the system, and C_{io} is the primary particle concentration.

Proceeding to dimensionless and normalised dependent variables and also boundary conditions, making use of the dimensionless parameters of **Eqs. (40) – (42)** (Oke et al. 2019).

Dimensionless position variable, $\eta = \frac{r}{R_o}$ (40)

Dimensionless time variable, $\tau = \frac{D_1 t}{R_o^2}$ (41)

Dimensionless concentration, $C = \frac{C_t - C_e}{C_0 - C_e}$ (42)

The initial and boundary condition changes, results to **Eq. (43) – (45) .**

$$C(\tau = 0, \eta) = 1 \quad (43)$$

$$C(\tau, 0) = 0 \quad (44)$$

$$C(\tau, 1) = 0 \quad (45)$$

Then, substituting the dimensionless variables into **Eq. (36)** results to **Eq. (46):**

$$\frac{\partial C}{\partial \tau} = \frac{\partial^2 C}{\partial \eta^2} \quad (46)$$

Eq. (46) predicts the speed at which particle is transfered at different operating conditions .

The method of separating variables was applied in solving the partial differential, **Eq. (46)**. It involves looking for a solution by which the time variable (τ) is parted from space variable (η) .

Then, reducing partial differential **Eq. (46)** to ordinary differential equation and applying the essential boundary conditions and also substituting all dimensionless parameters gives **Eq. (47)**

$$\frac{C_t - C_e}{C_0 - C_e} = 2 \sum_{n=0}^{\infty} \frac{1 - \cos n\pi}{n\pi}\ \left(\sin n\pi \frac{r}{R_0}\right) \left(e^{-(n\pi)^2 \frac{K_1 t}{16\pi r R_0^2}} \right) \quad (47)$$

Thus, expressing **Eq. (47)** as C_t, to define the concentration of particles in the system at some process time t, we have **Eq. (48)** .

$$C_t = C_e + 2\,(C_0 - C_e)\sum_{n=0}^{\infty}\frac{1-\cos n\pi}{n\pi}\ \left(\sin n\pi\frac{r}{R_0}\right)\left(e^{-(n\pi)^2\frac{K_1 t}{16\pi r R_0^2}}\right) \quad (48)$$

As a result, **Eq. (48)** represents the model equation that can predict the amount of colour particles transfer in the wastewater at any given process time.

where, $C_t$is the particle concentration at process at time, t; C_0 is the initial particle concentration at process at time, $(t) = 0$; and C_e is the equilibrium particles concentration at equilibrium time.

The model **Eq. (48)** was confirmed using MATLAB 9.3 software at different contaminant concentrations during the process occurring at different operating time. MATLAB 9.3, proved to be a great code-based mathematical and engineering package used for solving numerous mathemathical problems (Oke et al. 2021). The accuracy of the model was checked using the mean relative percentage deviation modulus $(\%M)$, of **Eq. (49)**. Thus, it explains the mean deviation of the predicted data from experimented data (Oke et al. 2014).

$$\%M = \left[\sum_{n=1}^{n}\frac{|M_{exp} - M_{pre}|}{M_{exp}}\right] x\ \frac{100}{N} \quad (49)$$

where M_{exp} = experimental data and M_{pre} = predicted data

From the $M\%$ analysis, values less than 5 confirmed an extremely good fit; then, $M\%$ values between 5 and 10 denote reasonably good fit; also, values above 10 showed poor fit . Additionally, some statistical tools such as: coefficient of determination (R^2), Chi-square (χ^2), F-test, and T-test were futher applied to the model testing using Microsoft Excel 2010.

2.7 Adsorption Mechanism Kinetics Study

Due to the cationic nature of the polymeric coagulants, adsorption mechanism played a enormous role in the coagulation-flocculation process. As a result, adsorption amount, adsorption equilibrium and adsorption kinetics studies were determined in order to ascertain the adsorptive nature of the coagulants used (Apua 2025; Hu et al. 2021; Onukwuli and Obiora-Okafo 2019). Adsorption capacity or adsorption amount (q_t) is used to study the extent of adsorption mechanism. However, the particle removal by coagulation-flocculation occurs via various mechanisms; first, by charge neutralisation, which involves the destabilisation of hydrodynamic particles which may be governed by physic-chemical interactions between the positively charged polymer molecules (cations) and negatively charged contaminants (anions). As a result, coagulants-contaminant complexes are formed, followed by flocs growth by adsorption mechanisms. An earlier study by Hu et al (Hu et al. 2021), found the adsorption capacity, q_t a suitable evaluation parameter for analyzing the extent of flocs growth. Adsorption capacity at any given time was solved according to **Eq. (50)** (Chowdhury et al. 2021).

$$q_t\,(\frac{mg}{g}) = \frac{(C_o - C_t)\,V}{M} \quad (50)$$

where C_o is the concentration of particles at $t = 0$ (mg/L), C_t is the concentration of particles at any specified time t (mg/L), V is the solution volume (L), and M is the mass of the coagulant (mg/L).

In order to study the rate at which the particles are transferred before adsorbing to the polymer surfaces, adsorption kinetics were studied. The study provides knowledge of the controlling mechanism of the process which governs mass transfer and the process time. Following the adsorption studies, the kinetic data were analysed using Pseudo first-order model, Pseudo second-order model and Elovich models.

Pseudo first-order model equation as initially proposed by Lagergren is in the form of **Eq. (51) (Apua 2025)**.

$$\log\,(q_e - q_t) = log q_e - \frac{K_{f1}}{2.303t} \quad (51)$$

where q_t is the adsorbate amount adsorbed at any time t (mg/g), q_e is the equilibrium adsorption capacity (mg/g), k_{f1} is the rate constant for Pseudo first-order kinetics (min^{-1}), and t is the process time (min).
Pseudo second-order equation as represented in **Eq. (52) (Apua 2025)**, usually predicts the particle behaviour throughout the process with chemisorption being the rate controlling step.

$$\frac{t}{q_t} = \frac{1}{k_2 q_e} + \frac{1}{qe}\, t \qquad (52)$$

where k_2 is rate constant for the Pseudo second-order ($gmg^{-1}min^{-1}$). The adsorption rate at the onset is represented by h ($mg^{-1}\ min^{-1}$) at $t = 0$, shown as **Eq. (53)**.

$$h = k_2 q_e^2 \qquad (53)$$

Then, Elovich kinetic (Apua 2025) model is among the useful models describing chemisorption processes. It is defined as **Eq. (54)**.

$$q_t = \frac{1}{\beta}\ln(\alpha\beta) + \frac{1}{\beta}\ln t \qquad (54)$$

where α is the initial sorption rate ($mgg^{-1}min^{-1}$) and β is the extent of surface coverage and also the energy of activation for chemisorption (gmg^{-1}). The value of $(\frac{1}{\beta})$ shows the available number of adsorption sites whereas $\frac{1}{\beta} ln(\alpha\beta)$ indicates the adsorption amount when ln t = 0. The appropriateness of the kinetics models to define the adsorption process was certified by the normalised standard deviation, Δq (%), given by **Eq. (55)** (Obiora-Okafo et al. 2014).

$$\Delta q(\%) = 100\sqrt{\frac{\sum[(q_{exp} - q_{cal})/q_{exp}]^2}{d_f}} \qquad (55)$$

where, d_f represents the degree of freedom of the equation. q_{exp} (mg/g) and q_{cal} (mg/g) represent the experimental and calculated adsorption capacities, respectively.

3.0 Results and Discussion

3.1 Characterization Results

3.1.1 Proximate study

Proximate analysis of the precursors as summarized in **Table 2** shows high moisture values indicating the coagulants' ability to absorb water, as well as, dissolves colour particles suspended in water (Obiora-Okafo and Onukwuli 2018a). High crude protein contents as recorded indicate the presence of active coagulation components. The values obtained shows an agreement with the literature that the protein contents of the precursors are cationic poly-peptides (Igwegbe et al. 2021a). Fibre contents present, established that the precursors were organic polymers having some visible tails and loops when dispersed in aqueous medium . The proximate results validate the use of the seed extracts as potential coagulants in this study. Similar biocoagulant characteristics has been reported Choudhary et al (Choudhary and Neogi 2017).

Table 2. Proximate characteristics of the proposed coagulants

S/No.	Parameters	Values	
		Brachystegia eurycoma (BE)	*Vigna subterranean* (VS)
1.	Yield	28.31	14.6
2	Bulk density (g/mL)	0.235	0.241
3.	Moisture Contents (%)	7.25	10.0
4.	Ash contents (%)	3.48	2.97
5.	Protein contents (%)	19.77	18.15
6.	Fibre contents (%)	2.20	1.64

7.	Carbohydrate (%)	56.76	60.94
8.	Fat contents (%)	10.53	6.30

3.1.2 FTIR analysis of the coagulants

The spectra representation of BEC and VSC are shown in **Figs. 5a-b**, respectively. In **Figs. 5a** there is a slight absorption peak of 3965.52 - 3780.36 cm^{-1} attributing to the stretching vibration of –OH, and the vibration of water absorbed (Igwegbe et al. 2021a). Also, the –OH groups with a peak at 3070.58 cm^{-1} were also evidenced in **Fig. 5b**. The free hydroxyl groups present confirms the occurrence of the free hydroxyl of carboxylic acids, alcohols and phenols in the coagulants. This band also corresponds to the O-H vibrations of cellulose, pectin and lignin. Consequently, there is an agreement between the results of **Table 2** and the spectral results indicating the presence of moisture (water), oil and carbohydrate (glycerides). Futhermore, the studies revealed that the absorption peak for the amines was evidenced in 3348.32 cm^{-1} for aliphatic primary amine (N-H) and secondary amine of 3070.58 cm^{-1} for BEC and VSC respectively. Also, the presence of N-H stretching signals detects the presence of amino compounds, confirming the presence of protein contents in the coagulant as demonstrated in **Table 2**. In addition, a major band in the broad region of 2021.34 cm^{-1} and 2052.20 cm^{-1} indicates the existence of a C=O group (carbonyl compound). There was also a strong adsorption peak at 694.36 cm^{-1} and 632.64 cm^{-1} for BEC and VSC respectively, showing the characteristic frequency for C-H out of plane deformation groups which is typically relative to the location and spatial geometry of the double bond (Zhao et al. 2020). Finally, the presence of moisture, proteins, and esters is confirmed by the FTIR spectral of BEC and VSC, as well as the proximate analysis provided in **Table 2**, justifying their usage as good sources of coagulants in this research.

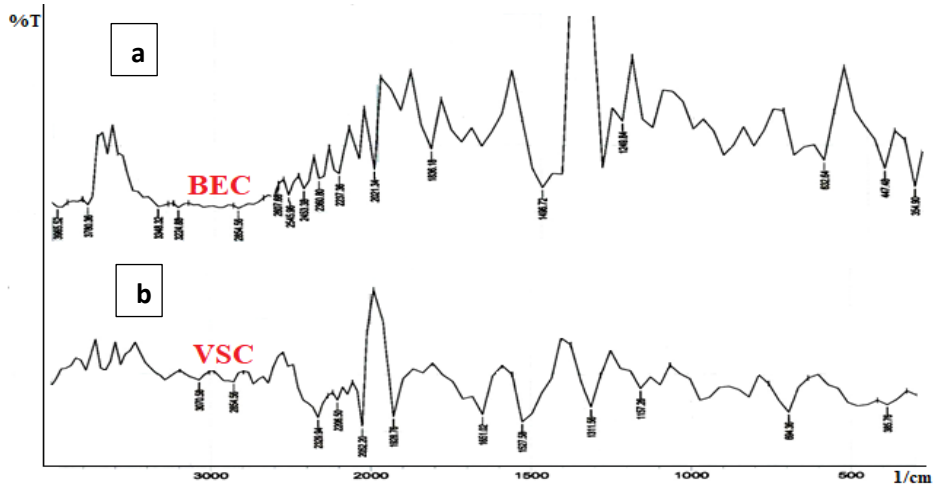


Fig. 5. FTIR Spectra of (a) BEC and (b)VSC

3.1.3 Morphological analysis of the coagulant

SEM was used to examine the surface morphologies of the coagulants in this investigation, as shown in **Fig. 6** at 600x magnifications. The 3D reconstructed SEM images revealed well-developed pores of various sizes and shapes. As a result, pore sizes (micro-pores, macro-pores, and meso-pores) and their distributions are unique to natural organic polymers (NOPs). Therefore, major pore size of 0.41 μm^2 was revealed in the histograms, as well as fibre lengths between 1.66-21.45 µm and 2.11-17.94 µm for BEC and VSC respectively as shown in **Fig. 7**. Varying fibre lengths are unique features of NOPs that enhances their multifunctional utilisation as coagulants and adsorbents (Obiora-Okafo et al. 2018). In addition, fibre length indicates that the mechanisms of the NOPs with such characteristics are via adsorption and sweep flocculation mechanism. Rough surfaces reveal that the coagulants are coarse fibrous solids primarily made of cellulose and lignin, indicating that they are polymeric. The binding of particles to polymer chains via inter-particle bridging or electrostatic interactions improves sweep flocculation. Adsorption as a crucial mechanism in the coagulation-flocculation process is also confirmed by holes and rough surfaces seen on the coagulant morphologies (Igwegbe et al. 2021a; Obiora-Okafo et al. 2018). Furthermore, morphologies also possess compact-net structures which are more conducive to particle flocculation owing to bridge

aggregation. Finally, when compared to the branching structure, the compact-net structure is better for flocculation and particle-bridge creation among flocs (Cao et al. 2017).

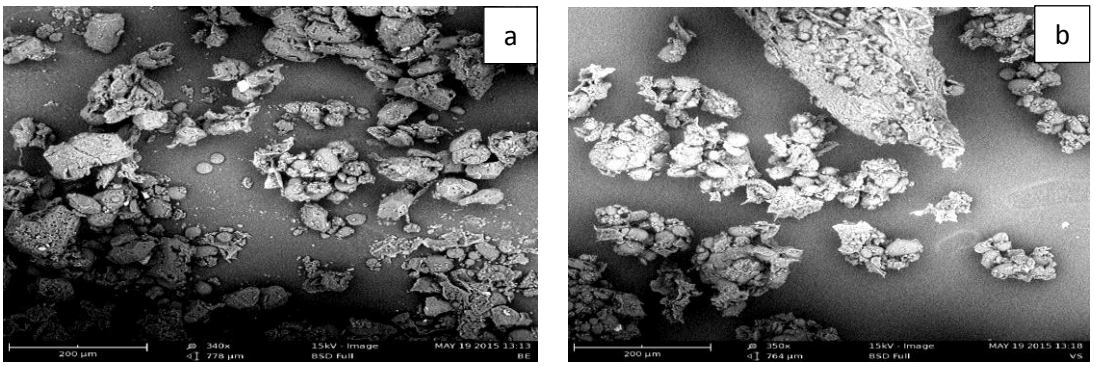


Fig. 6. SEM micrographs for (a) BEC and (b) VSC (600× magnifications)

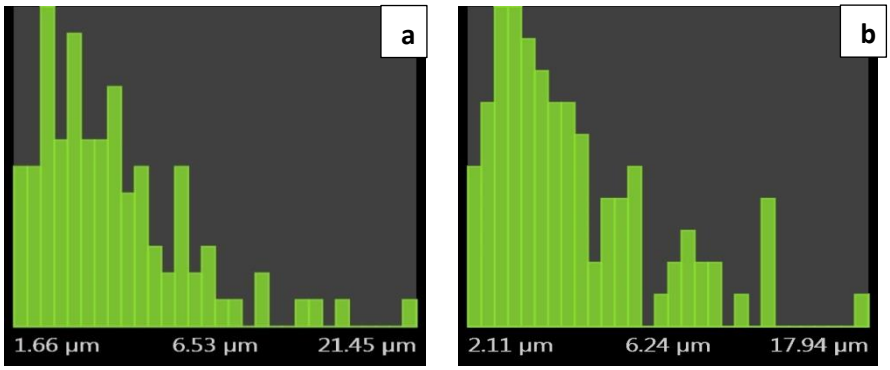


Fig. 7. Fibre lengths from SEM micrographs for (a) BEC and (b) VSC (600× magnifications)

3.2 Colour Removal and Colour Removal Efficiency as a Function of Settling Time

The flocculation process involves particle interactions and a time-dependent interface of coagulant hydroxide precipitate following the hydrolysis reaction (Liang et al. 2016; Obiora-Okafo et al. 2018). The time dependent effect of colour concentration and its removal efficiency are shown in **Fig. 8**. The percentage reduction in concentration as observed in 200 mgBEC/L and 200 mgVSC/L result to 97.7% at 480 min and 82.0% at 420 min respectively. In addition, the sharp reduction within 30 min specifies a speedy coagulation process that discloses the probable coagulation time (T_{ag}). Moreover, this rapid reduction in concentration may perhaps be attributed to either charge neutralisation or its combination with sweep flocculation mechanism (Cainglet et al. 2020). As a result, after 30 mins, the amount of particles accessible for flocculation diminishes, showing a gradual drop in colour concentration as the process progresses. This is most likely due to intricate coagulation-flocculation mechanisms that may include the development of a net-like structure that does not take a long period. Therefore, the greater flocculation time could be related to the presence of a sorption mechanism that necessitates a longer process time. After 300 min, there was no noticeable change in concentration, indicating that equilibrium has been reached. As a result of the saturation of the active adsorption sites, the aggregate becomes destabilized, preventing further adsorption and, as a result, the settling period is prolonged. For these reasons, coagulation-flocculation using NOPs in wastewaters is more efficient at low pH conditions (Cainglet et al. 2020).

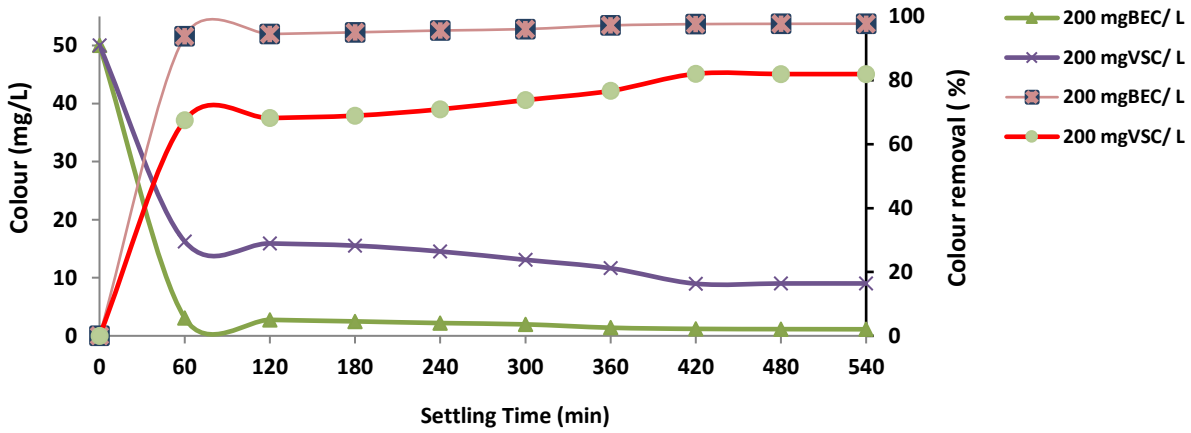


Fig. 8. Plots of colour removal and effect of settling time on the colour removal (%) from AR 66 dye. pH = 2, dye concentration = 10 mg/L, temperature = 303K.

3.3 Coagulation-Flocculation Kinetics Representing Brownian Motion

Analysis was performed on a 95% confidence level to determine the order of coagulation-flocculation response, and the parameters obtained from the regression analysis for BEC and VSC are provided in **Table 3**. The intercept and slope of the equation defining the kinetics of aggregation were used to calculate the coagulation rate constant, K, and the order of reaction (Eq. 3). The coagulation The proportionality constant that connects the reaction rate to the concentration of the reacting species is known as the coagulation rate constant. This implies that each minutes, 0.0165 mg/L and 0.000176 mg/L of colour particles were consistently attached to the polymer surfaces creating larger aggregates for BEC and VSC, respectively. From the calculation, the reaction order values obtain was in agreement with the conventional theory of coagulation-flocculation being a second-order process . Hence, the order of reaction gotten confirms the optimum order for the process, showing approximately second-order reaction. Also, the correlation coefficient (R^2) demonstrates good agreement that implies that the studied kinetic data is significant. T_{ag} is inversely proportional to the starting concentration of colour particles, suggesting that the higher the contaminant concentration, the shorter the coagulation time required for elimination (Obiora-Okafo et al. 2019). Furthermore, the collision efficiency (E) values explain the attainability assumption that particle collision between contaminants and coagulants is 100% efficient throughout the dispersion, implying that particles will stick together after bimolecular collision and that particle distribution or complex formation distribution will occur during the process as obtained by Ugonabo et al (Ugonabo et al. 2020).

Table 3. Coagulation Kinetics Parameters from Brownian Theory

Parameters	200mg BEC/L	200mg VSC/L
K (L/ mgmin)	1.65E-02	1.76E-04
A	1.2	2.2
R^2	0.985	0.991
Rate Equation (-r)	1.65×10^{-2} C^2	$1.76 \times 10^{-4} C^2$
T_{ag} (min)	22.42	27.92
K_1 (L/ min)	8.25E-03	8.78E-05
β (L/ mgmin)	0.0165	0.0001755
E (mg^{-1})	1.00	1.00

3.4 The Influence of Time on Particle Behaviour

Particles reduction behaviour as a function of time depicts the pattern at which colour concentrations are reduced. Figure 9 depicts the fluctuations in C_1, C_2, C_3 and C_4 for initially monodispersed particles obtained from Eqs. (27) - .(30), respectively. With increasing time, both the total colour concentration, C_t, and the concentration of the singlet

species, C_1, drop monotonically. The concentrations $C_{2\,(t)}$, $C_{3\,(t)}$ and $C_{4\,(t)}$ goes through a maximum since they are not present at the initial time and concentration (Ghernaout et al. 2015b). Because of an increasing number of particle concentration on aggregate formation over time, the number of singlets appears to be decreasing faster than the total number of particles . As a result of the bimolecular reaction, the total number of particles drops. Furthermore, we discovered that the lower the K value, the longer the coagulation time, giving rise to slow rate and longer coagulation-flocculation process .

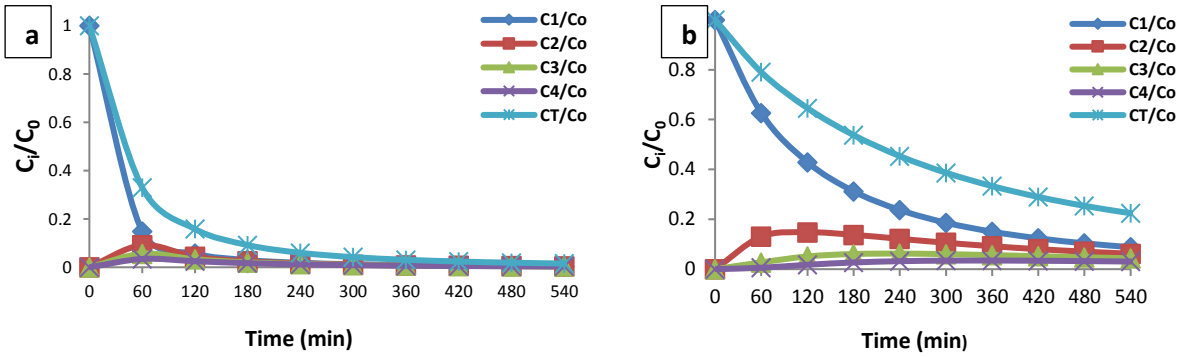


Fig. 9. The decrease in the normalised number of overall particles with time for colour removal using (a) BEC@ 480 min, and K = 1.65 x 10^{-2} mg/Lmin, (b) VSC @ 480 min and K = 1.76 x 10^{-4}mg/Lmin.

3.5 Adsorption Models

There is some attraction between polymer segments and particle surfaces during the flocculation process, which leads to adsorption . As a result, kinetic models such as Pseudo first-order, Pseudo second-order, and Elovich kinetic models were used to examine the rate at which particles are adsorbed onto polymer surfaces, as shown in **Fig. 10**. Thus, the kinetic parameters obtained were summarised in **Table 4**. Consequently, the R^2 for the models was quite low when compared to the Pseudo second-order model. Furthermore, the experimental data agrees well with the Pseudo second-order kinetic model data, with BEC and VSC having the lowest normalised standard deviation, Δq (%) values of 0.87 % and 2.24 %, respectively. Additionally, the coagulation-adsorption process is confirmed as a second-order process owing to an excellent fit of the Pseudo second-order kinetic model with R^2 of above 0.990. More importantly, the Elovich model's moderate agreement expanded our knowledge of the adsorption-chemisorption process, implying selective adsorption without site rivalry, as shown in organic polymers (Feng et al. 2021; Lanan et al. 2021), leading to the importance of the Langmuir model in the sorption process (Obiora-Okafo et al. 2018). Thus, chemisorption, which involves valence forces through electron sharing between polymers and pollutants, was found to affect the overall rate of the adsorption process (Ghernaout et al. 2015a).

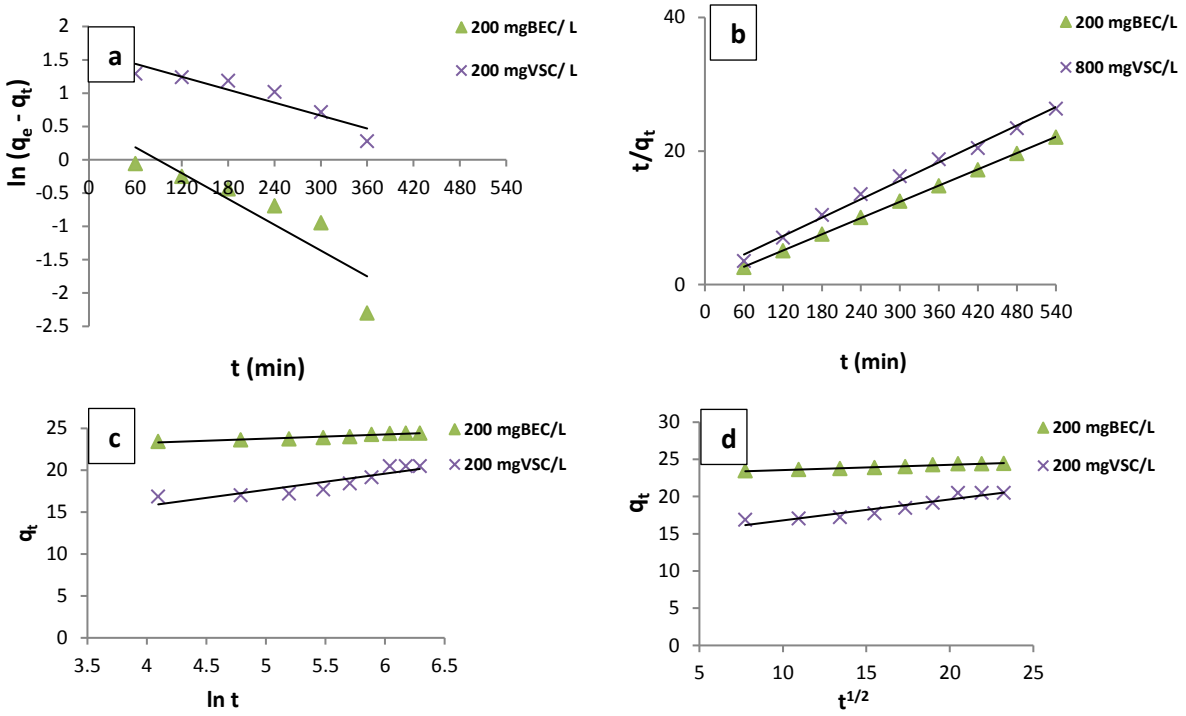


Fig. 10. The plot of adsorption kinetics showing: a. Pseudo first-order, b. Pseudo second-order and c. Elovich kinetics d. Intraparticle diffusion model.

Table 4. Adsorption model parameters for colour removal

Pseudo first-order kinetics					
	q_e, exp (mg/g)	**q_e, cal (mg/g)**	**K_{F1} (min^{-1})**	**R^2**	**Δq (%)**
200 mgBEC/L	24.4	1.361	0.007	0.828	33.38
200 mgVSC/L	20.5	5.119	0.003	0.863	26.53
Pseudo second-order kinetics					
	q_e, cal (mg/g)	**K_2 (g/mg min)**	**R^2**	**h (mg/g min)**	**Δq (%)**
200 mgBEC/L	25	0.173	0.999	10.16	0.87
200 mgVSC/L	21.74	0.0265	0.993	12.52	2.24
Elovich kinetics					
	A	**B**	**R^2**		
200 mgBEC/L	1.62E+07	2.004	0.926		
200 mgVSC/L	1.26E+02	0.52	0.800		

3.6 The Prediction of Particles Transfer Rate

The mass transfer rate was verified using particle concentration measurements that showed the experimental and projected particle transfer rates during the coagulation-flocculation process, as shown in **Fig. 11**. As a result, the projected results demonstrate that the rate of concentration reduction and, as a result, the rate of mass transfer was rapid at the start of the process, resulting in a tight agreement between the actual and expected results. Due to this, the anticipated equilibrium point is closer to the experimental equilibrium (Oke et al. 2021). **Table 5** displays the results of a statistical comparison of experimental and predicted data using the mean relative deviation modulus (*M%*), coefficient of determination (R^2), Chi-square (χ^2) test, F-test, and T-test. The lower the percentage, the better

the model prediction. The value of *M%* less than 10 indicates a good prediction of experimental data. Also, the correlation coefficient of the predicted results gave positive correlation values of 0.996 and 0.976 for BEC and VSC respectively. Furthermore, the χ^2 values greater than 0.05 are more significant than those less than 0.05. During the coagulation-flocculation process, the projected contaminant particle reduction pattern is likewise similar to the earlier study done by Jimoda, Oke (Oke et al. 2021).

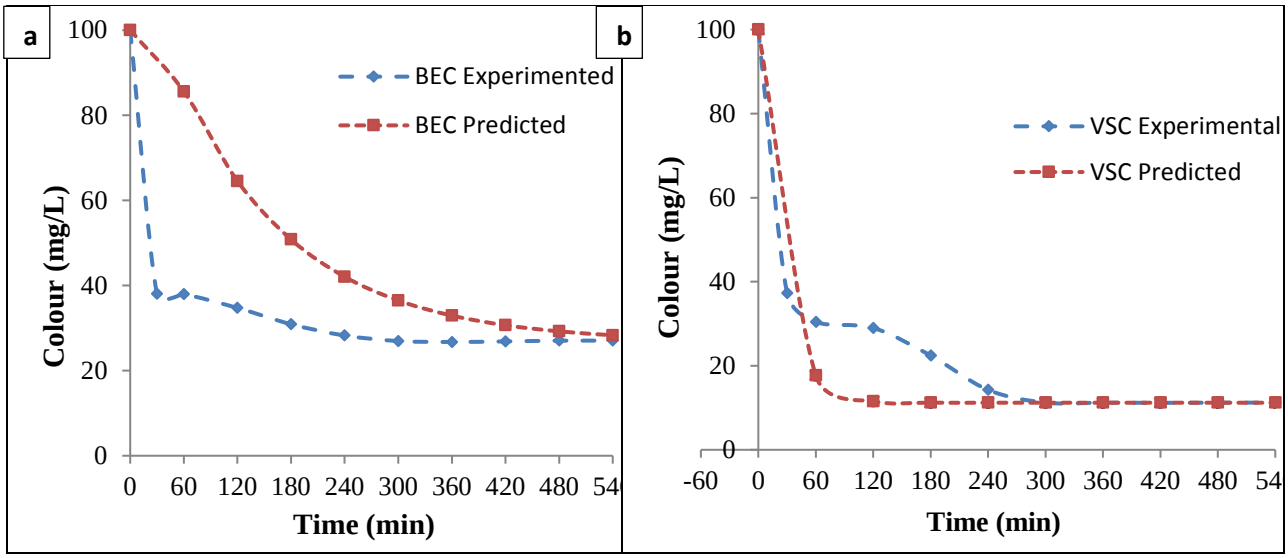


Fig. 11. Particle rate transfer through coagulation-flocculation process for; a. BEC and b. VSC.

Table 5. Confirmation result from the modelling

Coagulants	*M%*	R^2	χ^2	F-test	T-test
BEC	0.223	0.996	0.034	0.980	0.739
VSC	1.829	0.976	6.717	0.865	0.0085

4.0. Conclusion

The performances of the bio-coagulants for colour removal from simulated wastewater were studied. The NOPs employed, were found to be effective at removing colour from the simulated aqueous solution. The proximate, FTIR and SEM fibre metric analysis done on the coagulants showed that BEC and VSC have the coagulant and adsorption properties. The results also revealed the coagulant's ability to destabilize contaminant particles due to their cationic nature, adsorb particles on its surfaces, enhance floc formation due to their polymer characteristics, and then enhance large settleable flocs due to particle bridging and sweep flocculation mechanisms. Operational parameters studied (pH, coagulant dosage, dye concentration, settling time, and temperature) significantly influenced the colour removal process. The coagulation-flocculation study showed a time-dependent process and was incomplete without an adequate knowledge of the kinetics.The obtained values of K and α agreed with the traditional assumption that rapid coagulation is a second-order process. The adsorption process was more of a second-order process, demonstrating that the rate is proportional to the square of the particle concentration. These findings further suggested that the overall coagulation and adsorption were second-order processes governed by the chemisorption mechanism. Modelling showed a close agreement between the experimental and predicted particle reduction rate. It demonstrated a satisfactory prediction with *M*% values of less than 10%. The model investigated might be used to control colour particle transfer at any given condition, forecasting the rate of particle transfer in a process without requiring an experimental procedure. In addition, it could be used to extrapolate space and time that are not stated by the experimental results. Moreover, the coagulation-flocculation and adsorption capabilities of BEC and VSC were accredited with their efficiencies in the process. In conclusion, this NOPs could be applied in anionic dye containing wastewater treatment in Nigeria textile industries and its related, thereby reducing the usage of inorganic chemical coagulants. Also, the mass transfer model was used to predict the decreasing rate of contaminant particles concentration during the coagulation-flocculation process following good predictions of experimental data obtained

in statistical analysis. The model will improve and optimizes the design of equipment for the process and developing a clearer perception into the working of this coagulation-flocculation process.

5.0 Recommendation

Natural plant-based cationic coagulants can be successfully mass produced in Nigeria for colour removal using the extraction method adopted in this study due to its high efficiency delivery and less sludge production. The study on the particle mass transfer equation could be considered as a basis model employed to improve and optimize the design of process equipment for coagulation-flocculation process.

Acknowledgements

The authors would like to acknowledge the Department of Chemical Engineering, Nnamdi Azikiwe University, Awka, Nigeria and Energy Research Centre, University of Nigeria, Nsukka, Nigeria for making available their facilities for this study.

Nomenclature

APHA: American Public Health Association
AR 66: Acid red 66
AWWA: American Water Works Association
α: Coagulation order
b: Langmuir constant.
BEC: *Brachystegia eurycoma* coagulant
C_e: Equilibrium contaminant concentration (mg/l)
C_o: Initial contaminant concentration (mg/l)
C_{tot}: Concentration of total particles (mg/l).
C_1: Concentration for singlet particles (mg/l).
C_2: Concentration for doublet particles (mg/l).
C_3: Concentration for triplet particles (mg/l).
C_4: Concentration for quadruplet particles (mg/l).
d_f: Degrees of freedom
D_{ij}: Brownian diffusion coefficient
E_{ij}: Efficiency factor for collision between i and j-particles.
f_{ij}: Rate of collisions between particles of size i and j.
FTIR: Fourier transformed infrared
h_o: Initial adsorption rate h_o
I: Flux of diffusing species
KDa: Kilo Dalton
K_F: Freundlich constant
K_{F1}: Pseudo-first order rate constant
K_L: Langmuir constants
K_1: Von Smoluchowski rate constant for rapid coagulation
K_2: Pseudo-second order rate constant
K_3: Intra-particle diffusion rate constant
m: Coagulant mass (mg)
MCL: Maximum contaminant level
MW: Molecular weights
n: Freundlich constant
NOP: Natural organic polymers
q_e: Equilibrium adsorption capacity
q_{max}: Maximum contaminant concentration adsorbed per unit mass of coagulant, (mg/g).
q_t: Amount adsorbed at time, t.
Δq: Normalized standard deviation
R: Universal gas constant.
R^2: Correlation coefficient
R_L: Dimensionless Hall separation factor

R_{ij}: Particles radii
(-r): Rate equation
SEM: Scanning electron microscopy
t: Time (min)
T: Temperature (K)
T_{ag}: Coagulation-flocculation time
UV: Ultra violet
VSC: *Vigna subterranean* coagulant
WEF: Water Environment Federation
WHO: World health organization
λmax: Maximum absorbance

References

Apua MC 2025 Kinetics of adsorption of pollutants removal from mine wastewater by a coal fly ash-based coagulant International Journal of Environmental Engineering 13:57-91

Atoyebi JO, Osilesi O, Adebawo O, Abberton MT 2017 Evaluation of nutrient parameters of selected African accessions of Bambara groundnut (Vigna subterranea (L.) Verdc.) American Journal of Food and Nutrition

Aviara NA, Ibrahim EB, Onuoha LN 2014 Physical properties of Brachystegia Eurycoma seeds as affected by moisture content International Journal of Agricultural and Biological Engineering 7:84-93

Bal V 2020 Coagulation behavior of spherical particles embedded in laminar shear flow in presence of DLVO-and non-DLVO forces Journal of colloid and interface science 564:170-181

Cainglet A, Tesfamariam A, Heiderscheidt E 2020 Organic polyelectrolytes as the sole precipitation agent in municipal wastewater treatment Journal of Environmental Management 271:111002

Cao T, Sugimoto T, Szilagyi I, Trefalt G, Borkovec M 2017 Heteroaggregation of oppositely charged particles in the presence of multivalent ions Physical Chemistry Chemical Physics 19:15160-15171

Choudhary M, Neogi S 2017 A natural coagulant protein from Moringa oleifera: isolation, characterization, and potential use for water treatment Materials Research Express 4:105502

Chowdhury A, Kumari S, Khan AA, Chandra MR, Hussain S 2021 Activated carbon loaded with Ni-Co-S nanoparticle for superior adsorption capacity of antibiotics and dye from wastewater: kinetics and isotherms Colloids and Surfaces A: Physicochemical and Engineering Aspects 611:125868

Feng Q, Gao B, Yue Q, Guo K 2021 Flocculation performance of papermaking sludge-based flocculants in different dye wastewater treatment: Comparison with commercial lignin and coagulants Chemosphere 262:128416

Ghernaout D, Al-Ghonamy AI, Boucherit A, Ghernaout B, Naceur MW, Ait Messaoudene N, Aichouni M, Mahjoubi AA, Elboughdiri NA 2015a Brownian motion and coagulation process American Journal of Environmental Protection 4:1-15

Ghernaout D, Al-Ghonamy AI, Boucherit A, Ghernaout B, Naceur MW, Messaoudene NA, Aichouni M, Mahjoubi AA, Elboughdiri NA 2015b Brownian motion and coagulation process American Journal of Environmental Protection 4:1-15

Halimi RBMA 2020 Characterisation of the genetic variation in nutritional composition of bambara groundnut (Vigna subterranea (L.) Verdc.). Southern Cross University

Hu Y-y, Pan C, Zheng X, Hu F, Xu L, Xu G, Jian Y, Peng X 2021 Prediction and optimization of adsorption properties for Cs+ on NiSiO@ NiAlFe LDHs hollow spheres from aqueous solution: Kinetics, isotherms, and BBD model Journal of Hazardous Materials 401:123374

Hyrycz M, Ochowiak M, Krupińska A, Włodarczak S, Matuszak M 2022 A review of flocculants as an efficient method for increasing the efficiency of municipal sludge dewatering: Mechanisms, performances, influencing factors and perspectives Science of The Total Environment 820:153328

Ibrahim A, Yaser AZ, Lamaming J 2021 Synthesising tannin-based coagulants for water and wastewater application: A review Journal of Environmental Chemical Engineering 9:105007

Ighalo JO, Adeniyi AG, Igwegbe CA 2021 3D Reconstruction and Morphological Analysis of Electrostimulated Hyperthermophile Biofilms of Thermotoga neapolitana. Biotechnology Letters:1-7

Igwegbe CA, Onukwuli OD 2019 Removal of total dissolved solids (TDS) from aquaculture wastewater by coagulation-flocculation process using Sesamum indicum extract: effect of operating parameters and coagulation-flocculation kinetics The Pharmaceutical and Chemical Journal 6:32-45

Igwegbe CA, Onukwuli OD, Ighalo JO, Menkiti MC 2021a Bio-coagulation-flocculation (BCF) of Municipal Solid Waste Leachate using Picralima Nitida Extract: RSM and ANN Modelling Current Research in Green and Sustainable Chemistry 4:100078

Igwegbe CA, Onukwuli OD, Ighalo JO, Umembamalu CJ 2021b Electrocoagulation-flocculation of aquaculture effluent using hybrid iron and aluminium electrodes: A comparative study Chemical Engineering Journal Advances 6:100107

Ishak SA, Murshed MF, Md Akil H, Ismail N, Md Rasib SZ, Al-Gheethi AAS 2020 The Application of Modified Natural Polymers in Toxicant Dye Compounds Wastewater: A Review Water 12:2032

Kim S, Nam S-N, Jang A, Jang M, Park CM, Son A, Her N, Heo J, Yoon Y 2022 Review of adsorption–membrane hybrid systems for water and wastewater treatment Chemosphere 286:131916

Lanan FABM, Selvarajoo A, Sethu V, Arumugasamy SK 2021 Utilisation of natural plant-based fenugreek (Trigonella foenum-graecum) coagulant and okra (Abelmoschus escluentus) flocculant for palm oil mill effluent (POME) treatment Journal of Environmental Chemical Engineering 9:104667

Li R, Qi X, Wang W, Cheng M, Wang Y, Zhang P, Song G 2024 Floc Kinetics in Dual-coagulation for the Treatment of High-concentration Surfactant-kaolin Wastewater Journal of Polymers and the Environment 32:1706-1716

Liang L, Tan J, Peng Y, Xia W, Xie G 2016 The role of polyaluminum chloride in kaolinite aggregation in the sequent coagulation and flocculation process Journal of colloid and interface science 468:57-61

Ndagijimana P, Rong H, Duan L, Li S, Nkinahamira F, Hakizimana JC, Kumar A, Aborisade MA, Ndokoye P, Cui B 2024 Synthesis and evaluation of a novel cross-linked biochar/ferric chloride hybrid material for integrated coagulation and adsorption of turbidity and humic acid from synthetic wastewater: Implications for sludge valorisation Environmental Research 255:119134

Obiora-Okafo I, Omotioma M, Menkiti M, Onukwuli O 2014 Elimination of Micro Organic Particles from Wastewater Using Sawdust-Based Activated Carbon: Equilibrium, Kinetic and Thermodynamic Studies Int J Engr &Techn 14:95-102

Obiora-Okafo I, Onukwuli O 2018a Characterization and optimization of spectrophotometric colour removal from dye containing wastewater by Coagulation-Flocculation Polish Journal of Chemical Technology 20

Obiora-Okafo I, Onukwuli O, Eli-Chukwu N 2020 Evaluation of bio-coagulants for colour removal from dye synthetic wastewater: characterization, adsorption kinetics, and modelling approach Water SA 46:300-312

Obiora-Okafo I, Onukwuli O, Ezugwu C 2019 Application of kinetics and mathematical modelling for the study of colour removal from aqueous solution using natural organic polymer Desalin Water Treat 165:362-373

Obiora-Okafo IA, Onukwuli OD 2018b Characterization and optimization of spectrophotometric colour removal from dye containing wastewater by coagulation-flocculation Pol J Chem Tech 20:49-59

Obiora-Okafo IA, Onukwuli OD, Omotioma M 2018 The Relevance of Adsorption Mechanism on Spectrometric Colour Removal: Investigation of Optimum Operation Parameters Der Pharma Chemica 10:139-151

Oke E, Arinkoola A, Salam K 2014 Mathematical modeling of mass transfer rate during injection of CO2 into water and surfactant solution Pet Coal 56:54-61

Oke E, Okolo B, Adeyi O, Agbede O, Nnaji P, Adeyi J, Osoh K, Ude C 2021 Black-box modelling, bi-objective optimization and ASPEN batch simulation of phenolic compound extraction from Nauclea latifolia root Heliyon 7:e05856

Oke EO, Araromi DO, Jimoda LA, Adetayo Adeniran J 2019 Kinetics and neuro-fuzzy soft computing modelling of river turbid water coag-flocculation using mango (Mangifera indica) kernel coagulant Chemical Engineering Communications 206:254-267

Onukwuli O, Obiora-Okafo I 2019 Performance of polymer coagulants for colour removal from dye simulated medium: Polymer adsorption studies Indian Journal of Chemical Technology 26:205-215

Onukwuli OD, Obiora-Okafo IA, Omotioma M 2019 Characterization and colour removal from an aqueous solution using bio-coagulants: Response surface methodological approach Journal of Chemical Technology & Metallurgy 54

Oyegbile B, Ay P, Narra S 2016 Flocculation kinetics and hydrodynamic interactions in natural and engineered flow systems: A review Environmental Engineering Research 21:1-14

Sonal S, Ugale D, Mishra BK 2021 Combining Surface Water with Mine Water to Improve the Removal of Natural Organic Matter by Enhanced Coagulation Mine Water and the Environment:1-12

Ugonabo IV, Onukwuli O, Ezechukwu C 2020 Deturbidization of Pharmaceutical Industry Wastewater Using Natural Coagulant: Response Surface Methodology Applied International Journal of Progressive Sciences and Technologies 22:258-267

Vivas EA, Castillo HSV, Acosta EG 2025 Physicochemical and Structural Characterization of Coffee Husks for Sustainable Applications in Biodegradable Materials Journal of Natural Fibers 22:2453489

Zhao C, Zhou J, Yan Y, Yang L, Xing G, Li H, Wu P, Wang M, Zheng H 2020 Application of coagulation/flocculation in oily wastewater treatment: A review Science of The Total Environment:142795